Optica Applicata, Vol. XXXIV, No. 3, 2004

Femtosecond laser-induced damage in dielectrics

YUFENG PENG, YAOLI WEI, ZHENLONG LV

College of Physics and Information Engineering, Henan Normal University,
Xinxiang, 453007, People's Republic of China; e-mail: yufengp@sohu.com

We present a new method to investigate the ablation phenomenon by a 100 fs, 1053 nm Gaussian laser pulse in fused silica and describe the different mechanisms of ablation in long pulse and ultrashort pulse lasers. A modified rate equation is used to numerically calculate damage in dielectrics. In addition, we examine the respective role of ionization and avalanche ionization in femtosecond laser-induced damage. We find that present results are in quantitative agreement with those of earlier study.

Keywords: femtosecond laser, ablation mechanism, damage threshold, electron number density.

1. Introduction

Laser-induced breakdown and damage in transparent dielectrics have been investigated extensively since the advent of high-power pulsed-lasers [1]–[5]. These lasers are uniquely characterized by their ultrashort pulse duration (from 10 fs to 1 ps) and extremely high intensity (10^{12}–10^{15} W/cm^2) [6]. Optical breakdown by ultrashort pulse laser in dielectrics presents an efficient method to deposit laser energy into materials that otherwise exhibit minimal absorption at low laser intensity. Compared with their relatively long-pulse counterparts, ultrashort-pulse lasers have many advantages for laser material processing, including negligible heat diffusion effects, absence of the liquid phase during material removal, minimal plasma absorption, and smaller laser fluences for processing, which makes them capable of producing high-quality features with high spatial resolution [7]. Additionally, in recent years, the structural alternations produced in transparent materials by ultrashort lasers have been used for micromachining, thin-film formation, and bioengineering applications. Understanding the mechanisms for optical damage may allow high-damage-threshold optics to be constructed for ultrashort laser systems.

Laser-induced breakdown results in damage to dielectrics in terms of three major processes: i) the excitation of electrons in the conduction band by impact and multiphoton ionization, ii) heating of the conduction band (henceforth free) electrons by the radiation, and iii) transfer of the plasma energy to the lattice [1], [4], [8], [9].

In a transparent dielectric, there is no linear absorption of the incident laser light, two nonlinear mechanisms are responsible for optical breakdown and material damage: photoionization and avalanche ionization [10]. These are two different mechanisms that play a role in this absorption; by these two nonlinear mechanisms, laser energy is deposited into the material by promoting electrons from the valence band to the conduction band. If the laser intensity is strong, a very high free electron density, *i.e.*, a plasma, of the order of 10^{21} cm^{-3}, is produced. This high density plasma strongly absorbs laser energy by free-carrier absorption, the reflectivity of the plasma at the critical density is only a few percent, the shock-like energy deposition leads to ablation.

Optical breakdown threshold is associated with a threshold electron number density *n*-th and can be predicted by solving the electron number density rate equation. Research on electron number evolution induced by ultrashort laser pulses has been reported [1], [5]. In order to describe the ablation phenomenon accurately, we decided to present a new model which includes a reduction in the number of free electrons due to diffusion and recombination to determine the evolution of the free electron number density in dielectrics medium exposed to laser pulses of 100 fs. Results based on electron production via photoionization, avalanche ionization and loss via diffusion and recombination are in quantitative agreement with earlier studies [1], [5], [11], demonstrating that we present an effective method to determine the time-resolved electron number density and predict damage threshold.

2. Electron number density evolution

The present work modifies the rate equation model based on STUART *et al*. [1], [5] by taking electron diffusion and recombination into account and use the expressions which are different from formulas of STUART *et al*. [1], [5] to describe evolution of the conduction band electron number density.

2.1. Nonlinear photoionization

Photoionization refers to direct excitation of the electron by laser field. Because a single photon of visible light does not have enough energy to excite an electron in a transparent material from the valence band to the conduction band, so nonlinear ionization occurs due to the simultaneous absorption of several photons by an electron, the ionization rate describes the probability for multiphoton absorption [10]. During multiphoton ionization, the number of absorbed photons simultaneously by an electron depends on the ionization potential of the material δ and the photon energy $\hat{}\omega$, the smallest number of the absorbed photons k satisfying $k\hat{}\omega \geq \delta$. In this regime, ionization rate depends strongly on laser intensity. Researchers used multiphoton ionization rate which was described as follows [1], [4], [5]:

$$W(I)_{\mathrm{MPI}} = \sigma_k I^k \tag{1}$$

where σ_k is the multiphoton absorption coefficient for absorption of k photons, I is the laser intensity. This is one case of photoionization which is at high laser frequencies limit (but still below that required for single photon absorption). While in the opposite limiting case, *i.e.*, low frequency and strong fields, photoionization describes the tunnel effect [8]. In the tunneling ionization regime, the electric field of laser suppresses the Coulomb well that binds a valence electron to its parent atom. If the electric field is very strong, the Coulomb well can be suppressed enough for the bound electron to tunnel through the short barrier and become free [10]. The tunneling rate scales more weakly with the laser intensity than the multiphoton ionization rate. Researchers [1], [4], [5] also point out that the multiphoton ionization term should be replaced by the tunnel ionization expression in a field stronger than ~100 MV/cm. Nevertheless, calculations including tunnel ionization have not been presented.

For a 1053 nm Gaussian laser pulse, the temporal pulse shape has the form:

$$I(t) = I_0 \exp\left(-\frac{4\ln 2 t^2}{\tau^2}\right) \tag{2}$$

where τ is the full width at half-maximum (FWHM) pulse duration. In this case, eight -photon absorption is the relevant process, but eight-photon absorption cross-section values were not available. So, STUART *et al*. [5] used evaluation of Keldysh's expression for the multiphoton absorption rate:

$$W(I) = 9.52 \times 10^{10} \times I^8 \ \text{cm}^{-3}\text{ps}^{-1} \tag{3}$$

where the intensity I is in TW/cm^2.

In order to describe the photoionization rate accurately, we use Keldysh's photoionization expression [8]

$$W_{\text{PI}}(E) = \frac{2\omega}{9\pi}\left(\frac{\omega m}{\sqrt{\gamma_1}\hat{}}\right)^{3/2} Q(\gamma, \chi) \exp\left(-\pi\langle \chi + 1\rangle \frac{\kappa(\gamma_1) - E(\gamma_1)}{E(\gamma_2)}\right) \tag{4}$$

where ω is the laser frequency, m is the reduced mass, κ, E are complete elliptic integrals of the first and second kinds, respectively, and

$$\gamma = \frac{\omega\sqrt{m\delta}}{eE},$$

$$\gamma_1 = \frac{\gamma^2}{1+\gamma^2},$$

$$\gamma_2 = \frac{1}{1+\gamma^2},$$

$$Q(\gamma, \chi) = \sqrt{\frac{\pi}{2\kappa(\gamma_2)}} \sum_{n=0}^{\infty} \exp\left\{-n\pi \frac{\kappa(\gamma_2) - E(\gamma_2)}{E(\gamma_1)}\right\} \Phi\left\{\frac{\pi}{2}\sqrt{\frac{2\langle \chi + 1\rangle - 2\chi + n}{\kappa(\gamma_2)E(\gamma_2)}}\right\},$$

$$\chi = \frac{2}{\pi}\frac{\delta}{\hat{\omega}}\frac{\sqrt{1+\gamma^2}}{\gamma} E\left\{\frac{1}{1+\gamma^2}\right\},$$

$$\Phi(z) = \int_0^z \exp\left(y^2 - z^2\right) \mathrm{d}y,$$

and $\langle z\rangle$ – the integral part of the number z.

Figure 1 shows the general trend for the photoionization rate predicted by Keldysh's model as a function of electric field for a wavelength of 1053 nm and

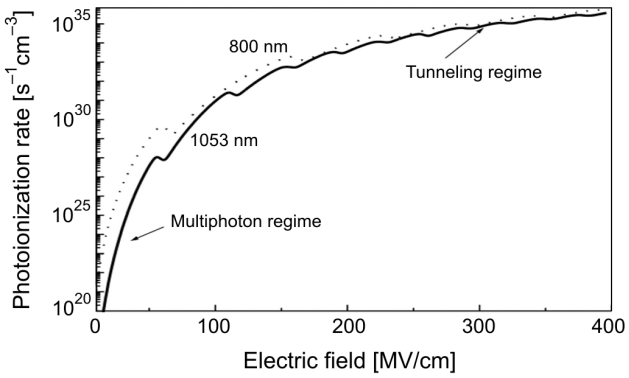

Fig. 1. Typical photoionization rate as predicted by Keldysh's model for a wavelength of 1053 nm (solid) and 800 nm (dotted).

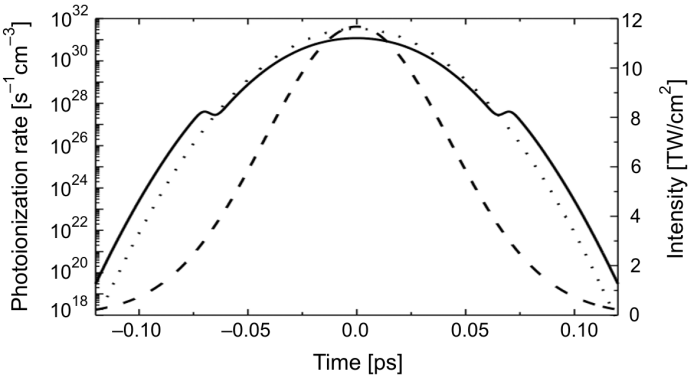

Fig. 2. Time dependence of Keldysh's photoionization rate (solid) and multiphoton ionization rate of STUART *et al.* [1], [5] (dotted) for a 1053 nm, 100 fs Gaussian laser pulse (dash).

800 nm. Time dependent Keldysh's photoionization rate and the multiphoton ionization rate based on the model of STUART *et al*. [1], [5] for a 1053 nm, 100 fs Gaussian laser pulse are presented in Fig. 2.

2.2. Avalanche ionization

Avalanche ionization is initiated when free electrons absorb laser energy through inverse Brehmstrahlung followed by impact ionization. Initial seed electrons originating from impurities or generated by ionization absorb several laser photons sequentially, moving to higher energy states in the conduction band [10]. During inverse Brehmstrahlung, seed electrons absorb laser photons by favour- able collisions with other electrons and ions. If the electrons sustain enough favourable collisions, they will eventually gain sufficient energy for impact ionization of other electrons, freeing new electrons to repeat the process. This avalanche ionization process results in a geometric increase in the free-electron density [12], [13].

STUART *et al*. [1], [5] suggest linear scaling of the avalanche rate with laser intensity, *i.e*., $\eta = \alpha I$ (α – the avalanche ionization coefficient), as shown in Fig. 3. Some researchers [3], [14] have called this model into question. The linear relationship between the avalanche rate and the laser intensity is the consequence of two major assumptions:

– flux doubling: an electron in the conduction band impacts ionization of an electron in the valence band as soon as it has enough energy to do so. In other words, there are no electrons in the conduction band with energy higher than the conduction band minimum plus the band-gap energy (at least until the material is fully ionized, after which further electron heating can occur);

– unchanged shape of electron distribution: the energy distribution of electrons in the conduction band does not change shape as the electron number density grows.

However, studies based on Monte Carlo methods conclude that in both semiconductors [15] and wide-gap materials [16], [17], the shape of the electron distribution is a

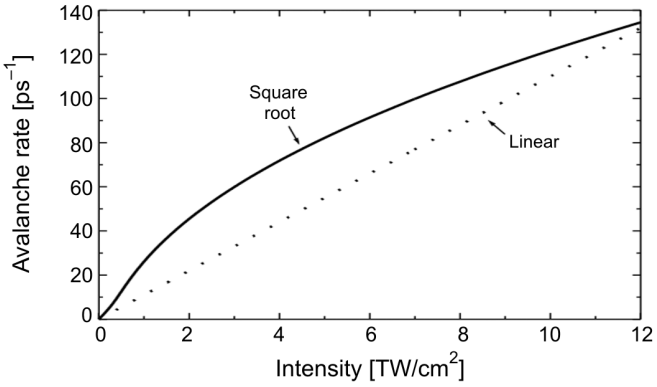

Fig. 3. Intensity dependence of avalanche rate based on Thornber's impact ionization (solid) and the model of STUART *et al*. [1], [5] (dotted).

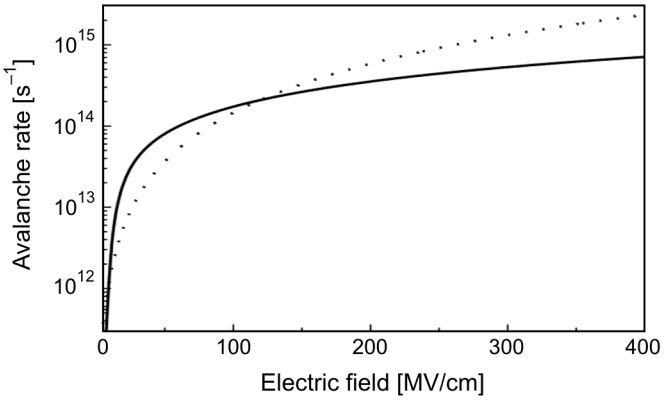

Fig. 4. Impact ionization rate based on Thornber's formula (solid) and avalanche rate of STUART *et al*. [1], [5] (dotted).

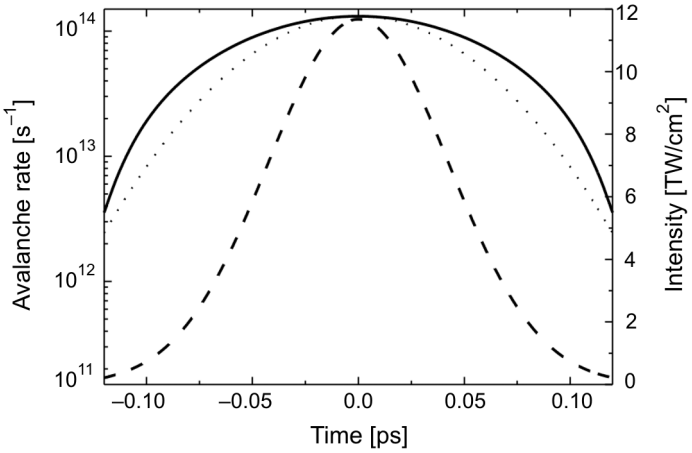

Fig. 5. Time dependence of Thornber's impact ionization rate (solid) and avalanche rate of STUART *et al.* [1], [5] (dotted) for a 1053 nm ,100 fs Gaussian laser pulse (dash).

function of the electric field and electrons can be found with energy greater than the ionization energy. Higher fields cause longer high-energy tails in the electron distribution. Therefore, the two assumptions are violated in a strong electric field.

We use Thornber's expression [18], [19] to describe the avalanche process which is applicable for all electric field strengths:

$$\eta(E) = \frac{v_{\text{drift}} eE}{\delta} \exp\left\{-\frac{E_I}{E(1 + E/E_{\text{phonon}}) + E_{KT}}\right\} \tag{5}$$

where v_{drift} is the saturate drift velocity. We denote E_{KT}, E_{phonon}, E_I as threshold fields for electrons to overcome the decelerating effects of thermal scattering, optical phonon scattering, and ionization scattering in one mean free path, respectively. Figure 3 depict intensity dependence of the avalanche rate based on Thornber's impact ionization and the model of STUART *et al*. [1], [5]. Impact ionization rate based on Thornber's formula and avalanche rate of STUART *et al.* as a function of electric field are plotted in Fig. 4. Figure 5 shows time dependence of Thornber's impact ionization rate and avalanche rate of STUART *et al*. for a 1053 nm, 100 fs Gaussian laser pulse.

2.3. Electron loss

As free electrons are formed in the conduction band through photoionization and avalanche ionization, two processes will contribute to reduction of electron population: diffusion and recombination.

The diffusion rate η_{diff} is given by [20]:

$$\eta_{\text{diff}} = \frac{\tau_0 \delta}{3m}\left[\left(\frac{2.4}{w_0}\right)^2 + \left(\frac{1}{z_R}\right)^2\right], \tag{6}$$

where the Rayleigh range

$$z_R = \frac{n_0 \pi w_0^2}{\lambda_0}, \tag{7}$$

where ω_0 – the beam waist, m – the rest mass of an electron, τ_0 – the mean free time between collisions, λ_0 – the laser wavelength in free space and n_0 – the refractive index of the medium. We use a Gaussian laser pulse for $\lambda = 1053$ nm with a beam waist $w_0 = 20$ μm irradiated on fused silica. This term is strongly dependent on the size of the focal volume, a small focal volume leads to higher electron diffusion. Unfortunately, accurate values of τ_0 have not been measured for most materials. Though, a value of 1 fs has been estimated by others [12], [20], and is used in our present work. As for the electron recombination rate, an empirical value $\eta_{\text{rec}} = 2\times10^{-9}$ cm^3/s as measured by DOCCHIO [21] is applied in this work, which is also used by others [12]. FAN *et al*. [22] also used this expression for the electron diffusion and recombination, further theoretical modeling of such a decay process needs to be done in the future.

2.4. Model for electron number density

A model for the evolution of electron number density is presented that takes the effects of photoionization, avalanche ionization, electron-ion recombination, and electron diffusion into account. The temporal behaviour of the free electron density n in the conduction band is described by the following equation:

$$\frac{\partial n}{\partial t} = \eta(E)n + W_{\mathrm{PI}}(E) - \eta_{\mathrm{diff}}n - \eta_{\mathrm{rec}}n^2, \tag{8}$$

where E is electric field, $\eta(E)$ is the avalanche rate described by Thornber's impact ionization, and $W_{\mathrm{PI}}(E)$ is the Keldysh's photoionization rate. The first two terms in Eq. (8) represent a gain of electron density. The last two terms in Eq. (8) refer to the loss in the number of free electrons due to diffusion and recombination. Since recombination requires two charged particles, it is proportional to n^2, on the other hand, electron diffusion depends linearly on n. This model was used by other authors [23]–[25]. By numerical evaluation of Eq. (8), we can determine the time-dependent electron number density and predict damage threshold.

3. Results and discussion

3.1. Electron evolution and material damage

In our calculation, we use a 100 fs, 12 TW/cm^2 Gaussian pulse which is described in Eq. (2) incident on fused silica. By numerical evaluation of Eq. (8) for the time-varying electron density, Fig. 6 depict the evolution of electron number density induced by femtosecond laser pulse; the electron number density produced by photoionization alone is included for reference.

From the figures, we find that photoionization strongly depends on intensity, therefore, the electron production takes place principally at the peak of the pulse. Only after the laser pulse is gone is energy transferred from the electrons to the lattices. In this 100 fs duration, multiphoton ionization produces a substantial amount of free electrons, material no longer has the properties of dielectrics, it becomes conductor,

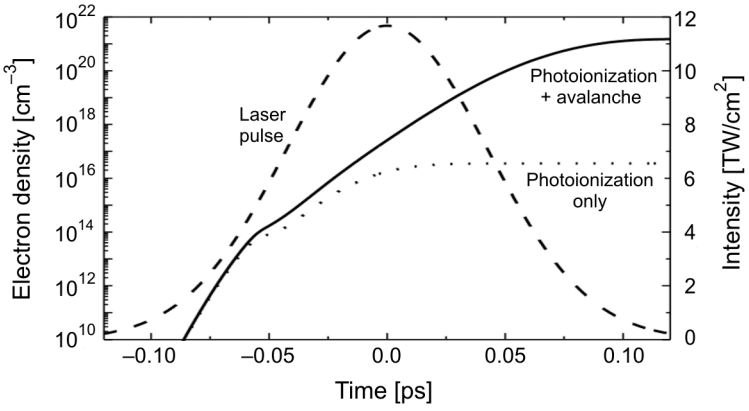

Fig. 6. Total (solid) electron number density and that produced by photoionization alone (dotted) plotted for a 1053 nm, 100 fs Gaussian laser pulse (dash).

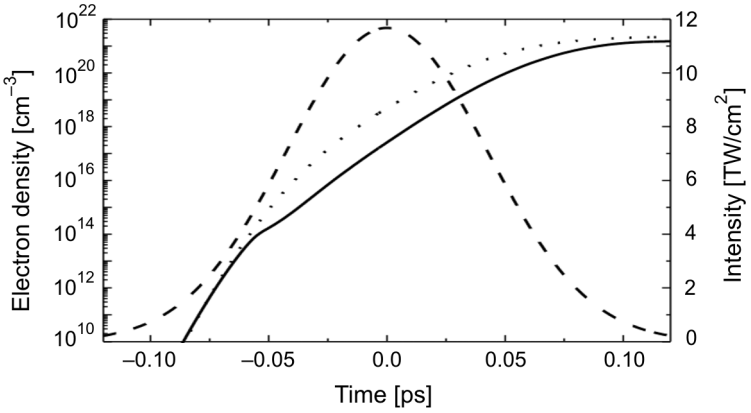

Fig. 7. Comparison of present work (solid) with results of STUART *et al.* [1], [5] (dotted) for a 100 fs, 1053 nm Gaussian pulse (dash) in fused silica.

and will absorb laser energy via inverse Bremstrahlung. So, the characteristic of laser –matter interaction becomes independent of the initial state of material, both dielectrics and metals have similar behaviour and morphology when machined with ultrashort laser pulses. For laser pulses of different duration, the relative fraction of photoionization to avalanche ionization will change, photoionization will contribute a relatively greater fraction of the electron number density with shorter pulses. Analyzing the figure, we find that avalanche ionization predominates even in the case of sub-100 fs pulses. If the laser field is high enough, photoionization rate reduces to the formula for the tunneling ionization, which alone produces the electron critical density n_{cr} to cause damage.

In order to validate the results derived from Eq. (8), comparison of our present work with the results of STUART *et al*. [5] for a 100 fs,1053 nm Gaussian pulse is depicted in Fig. 7. We can find that our present work is in quantitative agreement with the previous studies.

3.2. Mechanisms for long and short pulse

For sub-picosecond laser pulses, photoionization by the leading edge of the laser pulse provides seed electrons for avalanche ionization during the rest of the pulse. After seed electrons are produced, a small electron avalanche achieves the critical density plasma, this self-seeded avalanche makes short-pulse breakdown less dependent on defects in the material than long-pulse breakdown and therefore the threshold for short-pulse damage is deterministic. In this case, the electron-to-ion energy transfer time and the heat conduction time exceed significantly the pulse duration. Then the absorbed laser energy is going into the electron thermal energy, and the ions remain cold, making the conventional thermal expansion inhibited [26]. The energetic electrons created by the laser radiation pulled ions out of the materials. For pulses longer than a few tens of

picoseconds, energy is transferred from the laser-excited electrons to the lattice on a time scale of the pulse duration. This energy is then carried out of the focal volume by thermal diffusion. Thus, it is the relative rate of energy deposition and thermal diffusion that determines the damage threshold. Damage occurs when the deposited heat is sufficient to melt, boil, or fracture the dielectrics material [5], [10]. Simple calculations show that, in this case, the threshold fluence for optical damage scales as the square root of the pulse duration [23]. The source of the initial conduction band electrons that seed the avalanche ionization is very important for long pulse laser. Avalanche ionization is very efficient for such pulses because the long pulse duration allows more time for exponential growth of the electron density. Because avalanche ionization is so efficient, the laser intensity required to produce damage is not high enough to directly photoionizing electrons, so either thermally excited electrons or impurity and defect states provide the initial seed electrons for the avalanche. A high concentration of easily ionized impurity electrons lowers the threshold for optical damage compared to that of the pure material, making determination of the intrinsic breakdown threshold difficult [10], [19].

3.3. Uncertainty of the model

The loss term due to electron diffusion and recombination is not rigorous, other factors that cause a reduction in the electron population include energy loss from the pulse by scattering, linear absorption and nonlinear absorption, which are not included in the present model. During the breakdown process, plasma absorption dominates the energy loss and can dramatically alter the pulse profile, resulting in lower intensity. In addition, accurate mean-free time between collisions has not been measured for most materials. If these factors are taken into account accurately, higher peak intensity will be required in the model to produce the same critical electron density. Further theoretical model of ablation is needed to develop in the future.

4. Conclusions

In summary, ultrashort pulse laser has many advantages for many technologies. During optical breakdown, a high density of free electrons is formed in the material, which dominates energy absorption, and in turn, the material removal rate during ultrafast laser material processing. We present a new model to determine the time-dependent electron number density in fused silica by femtosecond laser. Keldysh's photoionization rate and Thornber's avalanche rate, in addition, a decay term due to free electrons diffusion and recombination are included in the new model. Based on the numerical evaluation of electron density, we examine the respective role of ionization, and avalanche ionization in ultrashort laser induced damage. In addition, ablation mechanism of dielectrics by femtosecond lasers is presented which is quite different from the thermal ablation by long pulses. Present results are in quantitative agreement with earlier study, demonstrating that we use an effective method to determine the produced electron number density and predict damage threshold.

References

[1] STUART B.C., FEIT M.D., RUBENCHIK A.M., SHORE B.W., PERRY M.D., Phys. Rev. Lett. **74** (1995), 2248; J. Opt. Soc. Am. B **13** (1996), 459.
[2] VAREL H., ASHKENASI D., ROSENFELD A., HERRMANN R., NOACK F., CAMPBELL E.E.B., Appl. Phys. A **62** (1996), 293.
[3] DU D., LIU X., MOUROU G., Appl. Phys. B **63** (1996), 617.
[4] LENZNER M., KRÜGER J., SARTANIA S., CHENG Z., SPIELMANN CH., MOUROU G., KAUTEK W., KRAUSZ F., Phys. Rev. Lett. **80** (1998), 4076.
[5] STUART B.C., FEIT M.D., HERMAN S., RUBENCHIK A.M., SHORE B.W., PERRY M.D., Phys. Rev. B **53** (1996), 1749.
[6] STRICKLAND D., MOUROU G., Opt. Commun. **56** (1985), 219.
[7] CHING-HUA FAN, JON P. LONGTIN, Appl. Opt. **40** (2001), 3124.
[8] KELDYSH L.V., Sov. Phys. JETP **20** (1965), 1307.
[9] MING LI, SAIPRIYA MENON, JOHN P. NIBARGER, GEORGE N. GIBSON, Phys. Rev. Lett. **82** (1999), 2394.
[10] SCHAFFER C.B., BRODEUR A., MAZUR E., Meas. Sci. Technol. **12** (2001), 1784.
[11] PERRY M.D., STUART B.C., BANKS P.S., FEIT M.D., YANOVSKY V., RUBENCHIK A.M., J. Appl. Phys. **85** (1999), 6803.
[12] NOACK J., VOGLE A., IEEE J. Quantum Electron. **35** (1999), 1156.
[13] KENNEDY P.K., HAMMER D.X., ROCKWELL B.A., Prog. Quantum Electron. **21** (1997), 155.
[14] AN-CHUN TIEN, STERLING BACKUS, HENRY KAPTEYN, MARGARET MURNANE, GERARD MOUROU, Phys. Rev. Lett. **82** (1999), 3883.
[15] YEOM K., JIANG H., SINGH J., J. Appl. Phys. **81** (1997), 1807.
[16] ARNOLD D., CARTIER E., Phys. Rev. B. **46** (1992), 15102.
[17] ARNOLD D., CARTIER E., DIMARIA D.J., Phys. Rev. B. **49** (1994), 10278.
[18] THORNBER K.K., J. Appl. Phys. **52** (1981), 279.
[19] DU D., LIU X., KORN G., SQUIER J., MOUROU G., Appl. Phys. Lett. **64** (1994), 3071.
[20] KENNEDY P.K., IEEE J. Quantum Electron. **31** (1995), 2241.
[21] DOCCHIO F., Europhys. Lett. **6** (1998), 407.
[22] FAN C.H., SUN J., LONGTIN J.P., J. Appl. Phys. **91** (2002), 2530.
[23] NIEMZ M.H., Appl. Phys. Lett. **66** (1995), 1181.
[24] BLOEMBERGEN N., IEEE J. Quantum Electron. **QE-10** (1974), 375.
[25] JIA T.Q., LI R.X., LIU Z., CHEN H., XU Z.Z., Appl. Surf. Sci. **189** (2002), 78.
[26] GAMALY E.G., RODE A.V., LUTHER-DAVIES B., Phys. Plasmas. **9** (2002), 949.

Received April 26, 2004